Canadian Water Resources Journal / Revue canadienne des ressources hydriques ›
Volume 37, 2012 - Issue 2

Research Paper

Spatial Snow Depth Assessment Using LiDAR Transect Samples and Public GIS Data Layers in the Elbow River Watershed, Alberta

Chris Hopkinson, Tim Collins, Axel Anderson, John Pomeroy & Ian Spooner

Pages 69-87 | Published online: 23 Jan 2013

Cite this article https://doi.org/10.4296/cwrj3702893

Abstra

This stud S
techniqu lume within
the m a. Two
LiDA e other
during la ing. These
data wer e snow
depth es valent land
classifica m 1675 field
measure h, 2008) in
snow-co now depth

0.18 m when averaged across both snow-covered and snow-free areas. Using field measurements of snow density, a GIS routine was employed to estimate total watershed snow water equivalent (SWE) from ten snow accumulation units (SAUs) using elevation, aspect and canopy cover. The total watershed SWE estimate was 46.0 106 m3. This volume of water can also be expressed as 0.058 m of water depth across the entire basin, or approximately 18% of the total 2008 runoff yield. Further work is needed to improve LiDAR-based snow depth estimation in areas of shallow snowpack where the influence of noise in the data is highest and to optimize the methods of sampling and extrapolation. At the present level of airborne LiDAR sophistication, positional uncertainties in LiDAR data (though small) are such that high confidence in the watershed snowpack volume estimate, would only be achieved during deep snowpack years; which also tend to be the years where accurate data are least required. However, given the availability of LiDAR base maps is ever growing, and the accuracy and costs associated with the technology are constantly improving, this approach to snow depth sampling has the potential to become a useful tool to support headwater snowpack resource assessment in water-stressed regions of Canada.

La prsente tude dmontre la possibilit d'utiliser la tldtection par LiDAR en combinaison avec des technologies SIG pour estimer le volume instantan du manteau neigeux en hiver dans la zone montagneuse d'Elbow River Watershed (bassin versant d'Elbow River) situe en amont de Calgary, Alberta. Deux ensembles de donnes LiDAR (dtection et tlmtri vers la fin de l'hive uche de neige. C rrain et du couvert eige dans des zone enne des 1675 me AR d'hiver (fin Mars La profo zones enneige m (= 1,2 m) soit 0,18 SIG utilisant des mes r lquivalent total en face du sol. L'estima bien tre exprim en comme

estimations base de LiDAR de lpaisseur de la neige dans des zones de manteau de neige peu pais o l'influence de bruit est la plus marque, et pour optimiser les mthodes dchantillonage et extrapolation. Au niveau actuel de sophistication du LiDAR aroport, des incertitudes de position dans les donnes LiDAR (quoique faibles) sont telles qu'un haut degr de confiance en l'estimation du volume de neige accumule dans le bassin ne serait ralis que pour les annes de neige profonde alors que, de faon gnrale, ce sont ces annes-l o le besoin de donnes prcises est moindre. Vu que les cartes ralises base du LiDAR sont de plus en plus disponibles et que les cots et la prcision des donnes associs cette technologie vont toujours s'amliorant, cette mthode dchantilloner lpaisseur de la neige est d'une utilit potentiellement trs souhaitable pour appuyer lvaluation des ressources en neige accumule du cours suprieur d'une rivire dans les zones de stress hydrique au Canada.

Introduction

In Southern Alberta's Bow River basin (BRB) (~26,000 km^2), most of the runoff originates as snowpack in the mountainous headwaters of the Canadian Rockies. The importance of water, and therefore snow, in this region where supply appears insufficie water allocatio mulations in the Bow at 20 snow course s d the potentia nt to provide an accur headwater snow co nat cont water availa characte

Global c more active precipita for the BRB (Martz e ularly forest canopy s d land use,

(Musselman et al., 2008; Winkler and Boon, 2010), thus altering any long term relationship. Given the likelihood for continued environmental and developmental changes in parts of the BRB (and other headwater supply regions), there is some uncertainty regarding the adequacy of snow course networks to provide reliable indices of future water availability. Consequently, there is a need to explore alternative snowpack monitoring methods, such as using remote sensing techniques (e.g., Derksen et al., 2005), that can more directly quantify total headwater snow pack accumulations.

Previous studies have demonstrated that snowpack depth variation can be assessed at the meso-scale with airborne LiDAR (Light Detection and Ranging) (Hopkinson et al., 2004; Deems et al., 2006; Fassnacht and Deems, 2006; Minoru and Hiroshi, 2006; Trujillo et al., 2007). In a study conducted over the Marmot Creek Watershed in the headwaters of the BRB it was found that LiDAR estimates of snow depth in alpine, forested slopes and valley locations demonstrated mean depths within 0.13 m of corresponding field data (Hopkinson et al., 2011). Alpine slopes demonstrated the highest accuracy, presumably due to reduced system error propagation (Goulden and Hopkinson, 2010), while forest-covered slopes demonstrated the highest uncertainty, likely due to signal interference by the overlying canopy and understory vegetation. Furthermore, the LiDAR snow depth model (LSDM) clearly illustrated that the watershed hypsometric mean snow depth reached its maxima at treeline around 2250 m a.s.l. (Hopkinson et al., 2011). [For an in depth introduction to the basics of airborne LiDAR technolo 1999).]

Given th ohic base map cov gary and the provinci ling strategy re to devise a minim he entire wate olation of snow s to sample the wate observations into disc controlling land sur ach is seen as a pot nce on empirica a more

Study Area

The ideal location to showcase LiDAR snow depth sampling would be an area of typically deep and widespread snow accumulation in the upper reaches of the BRB such as exist upstream of Banff or Lake Louise in Banff National Park. However, for this study the Elbow River Watershed (ERW) (Figure 1) was chosen for a number of strategic reasons: 1) The ERW (1210 km^2) drains into the Glenmore Reservoir (3.8 km^2), which supplies the City of Calgary (~1.1 million people) with ~24% of its drinking water (Pernitsky and Guy, 2008). The reservoir also acts to buffer spring flood waters and provide an important recreational capacity to the people of Calgary; 2) Unlike the protected National Park setting of the Upper Bow, the ERW experiences forestry operations at intermediate elevations and agricultural land uses in the lower reaches; 3) The government of Alberta Sustainable Resource Development department (SRD) monitor and inventory land use and forest cover within the ERW; 4) Provincially owned LiDAR base map coverage from a snow free period in 2006 was already available for approximately 40% of the ERW, whereas only a fraction of the Upper Bow was available from previous research-based data collections.

Figure 1. Elbow River Watershed (ERW) study area in Alberta showing field and LiDAR sampling

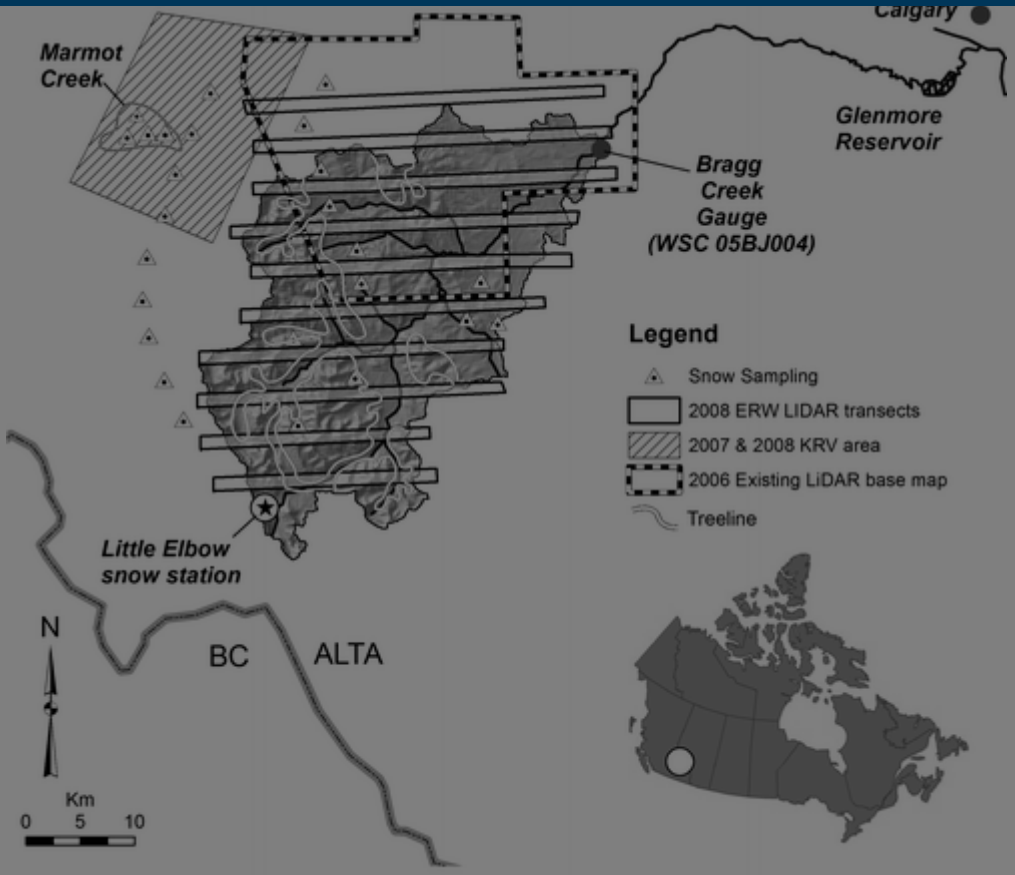

Figure 1. Elbow River Watershed (ERW) study area in Alberta showing field and LiDAR sampling locations. ERW area background illustrated as terrain shaded relief.

Display full size

Characteristic of the BRB in general, spring snowmelt from the ERW typically contributes the highest sustained period of inflow to the Glenmore Reservoir. Observed and modeled changes in the climatic regime over the ERW indicate increasing winter tempera s snow in the lowe gnitude of the ERW be modifie g back potentia Valeo et al., 2007). D valuable as it can in supplies at mini

Snow pr onment Canada da online climate essed February cal stations simultan ata. Howeve re are eight

currently operate one snow pillow and collect monthly snow course measurements during winter at the Little Elbow snow monitoring station. This station is located in the westernmost upper reaches of the watershed at 2225 m a.s.l. in an area of relatively high snowpack accumulation. Given most of the snowpack in the ERW is found in the mountainous headwaters of the basin, the LiDAR sampling study was carried out across the 790 km^2 area upstream of Bragg Creek hydrometric gauging site 05BJ004 (Water Survey of Canada) (Figure 1).

This paper reports on the field and LiDAR sampling strategy and the GIS methodology adopted to estimate snow depths within areas of the watershed that were outside the LiDAR sampling transects. It is not the intent of this paper to discuss in detail the process or results of LiDAR snow depth measurement and validation in a mountainous environment, as such analyses have been presented elsewhere (Deems et al., 2006; Fassnacht and Deems, 2006; Trujillo et al., 2007; Hopkinson et al., 2011). To support this project, however, complimentary LiDAR snow depth and land surface type SAU analyses conducted immediately west of the ERW along the slopes of the Kananaskis River Valley (KRV), which includes Marmot Creek watershed, are presented.

LiDAR Snow Depth Mapping

The Ch

The com DM) is to generate nd a digital surface (Hopkinson et al., 2

Clear surfaces. This lead need to be planned errain surface g; 2) The two acqu r of snow accumul possibility for terra he LiDAR

Canadian Rockies. For the ERW above Bragg Creek there was approximately 40% base LiDAR coverage, which was limited to the northern half of the watershed and the lower 1000 m of relief (Figure 1). The southern half and the upper 400 m of relief (or the upper 11% of basin hypsometry) are not represented. Within meso-scale mountainous watersheds, snow depth observations and simulations can vary widely as a result of different landcover and terrain features exerting variable levels of control (e.g., Elder et al., 1998). Therefore, if our sample set has no representation for the upper 400 m of the watershed, this constitutes a serious limitation. While it was not possible to directly represent this part of the ERW using publicly available LiDAR data, we were fortunate to have access to a research-based LiDAR dataset (DeBeer and Pomeroy, 2010; Hopkinson et al., 2011) collected over the Kananaskis River Valley (KRV) and adjacent slopes immediately to the west (Figure 1). The range in landcover and elevation of the KRV survey encompasses that of the upper westernmost headwaters of the ERW and thus provides a useful proxy.

In addition to spatial sampling challenges, collecting, processing and then comparing high resolution LiDAR surface models has many opportunities for error propagation (Hodgson et al., 2005; Deems and Painter, 2006; Goulden and Hopkinson, 2010). Therefore for each LiDAR surface there is a need to check for and reduce systematic positional bias and ensure comparable data resolutions prior to subtraction. While contemporary airborne LiDAR data accuracies are frequently quoted to be <15 cm (Optech
an occur
and so t
tures can be
necessa
n some
spatial b
nother
dataset,
DSMs are
created
uences do
not prop
n
mou
a vertical
error ov
et al., 2005).
In a stud
ported that
vertical
s due to a
horizont
06).
Complet
enging and
can requ
ely

be anticipated and addressed. If they are not, then the resultant LSDM change surface is likely to contain areas of systematic error that reflect properties of the underlying terrain and other uncertainties in the data.

LiDAR Data Preparation

Recognizing that airborne LiDAR monitoring has the potential to be costly over large areas, a sampling strategy was devised to minimize air time while representing a range of terrain and landcover attributes within the ERW. Two LiDAR datasets were required to perform the analysis; the first was collected as part of a Provincial base mapping initiative during snow-free and green foliage conditions in September 2006; while the second was commissioned specifically for this study during anticipated deep watershed snow accumulation. Both surveys were flown at an altitude of 3500 m a.s.l. using the same Airborne Laser Terrain Mapper (ALTM) 3100 sensor (Optech; Toronto, Ontario) owned and operated by Airborne Imaging Inc. based in Calgary, AB. In both cases, the pulse repetition frequency used was 33 kHz, and the average point spacing at ground level was between 1 m and 2 m, with actual point density increasing and swath width decreasing with terrain elevation. Sensor calibration and validation was performed before and after each flight at the Springbank Airport runway 20 km north-east of Bragg Creek and resulted in a vertical R.M.S. error less than 0.1 m.

The LiDAR DSM acquisition occurred on March 28th, 2008. Flight lines were flown in east to west t km for optimal w-free LiDAR coverag epresented, snow-fre tely to the west, we ng equivale as flown in summe ch (C-CLEA 08. The only differenc spatial coverag

Before s t the following

1. Grou

industry-standard TerraScan software (Terrasolid, Finland).

2. Horizontal and vertical co-registration of the snow-covered and snow-free LiDAR datasets. The two LiDAR point clouds were visually checked for spatial alignment in areas of no snow cover. Several profiles across the two datasets were extracted and compared throughout each transect to ensure spatial correspondence. Highway, building and cliff edge features were used to assist with the fine alignment of data.
3. The classified and corrected point cloud data were gridded to a 1 m resolution raster surface using a Triangular Irregular Network (TIN) interpolation procedure. This gridding technique was used as it maintains point position integrity and is less susceptible to artificial smoothing of break line features such as cliffs and gorges (Keckler, 1995).

Following creation of the bare ground DEM and snow covered DSM, the LSDM was generated in ArcMap (ESRI; Redlands, CA). A histogram of the LSDM grid node values was generated so that systematic biases could be identified and to enable subsequent snow depth summaries for certain land surface classes. Bin widths of 0.1 m were chosen for the snow depth increments, as this was close to the observed precision in the LSDM (Hopkinson et al., 2011). A snow free threshold of 0.05 m was used to minimize the number of cells erroneously classified as bare snow. This depth threshold resulted in a snow covered area of 70% for the transect areas sampled. The remaining 30% of t lustrating negative d that all negative all horizont d Demuth (2006) a me outlying behaviou all data associat from further anal ns from the LSDM ar le. In practice tal area sampled

Field Sampling

Field snow depths were sampled both in the ERW and in the KRV study areas over a five day period starting one day prior to the airborne LiDAR surveys and ending two days after. Within both the ERW and KRV the intent of the field campaign was to sample snow depths that were coincident with airborne LiDAR estimates while representing the range of elevation and canopy conditions experienced in ERW. Data from the more easily accessible KRV sites were a valuable supplement to the ERW analyses, as the terrain and land covers are similar to ERW so the SAU controls on relative accumulations are comparable. In practice, the KRV data were used to validate the LSDM approach, as flight lines over the ERW were offset from the field data due to a real time malfunction in the LiDAR navigation system. Consequently, the ERW field data were used to evaluate land surface type SAU influences on snow depth and to provide a comparative sample estimate of snow depth, instead of the intended correlative analysis.

Field data were collected at 25 spatially distributed sites (12 ERW and 13 KRV) at elevations ranging from <1300 m a.s.l. to >2300 m a.s.l. (see Figure 1) using either ground or helicopter transportation. At each of the sites, at least two profiles of nested snow depth measurements were made (Figure 2). Profile lengths varied from 25 m up to 100 m in length and five measurements of snow depth were made at every 5 m increme 1 m out from cer n the ERW and 139 d GPS to give app urement location GPS to provide LSDM estimate bulk snow uivalent (SWE 34 digital hemisph ach location could be ach field snow de l attributed with spa ls on depth and den mulation unit (SAU) pr

Figure 2. Optimal field snow depth sampling design. Four radial depth measurements were made one metre out from at each sampling location along each profile. Due to local terrain and land cover constraints, most field sample profiles at each site did not intersect at the midpoint and many were limited to a length of 50 m. Only the locations in the KRV underwent differential GPS positioning.

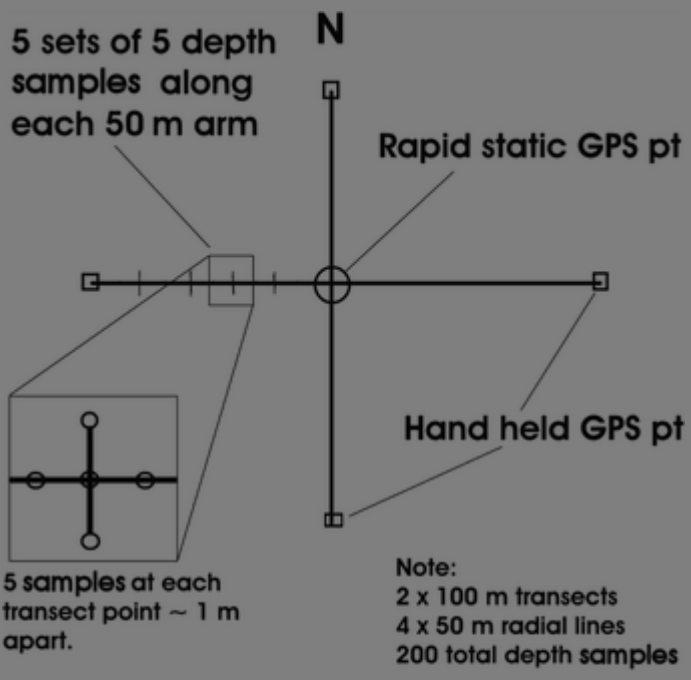

Figure 2. Optimal field snow depth sampling design. Four radial depth measurements were made one metre out from at each sampling location along each profile. Due to local terrain and land cover constraints, most field sample profiles at each site did not intersect at the midpoint and many were limited to a
KRV under

Display ful

Land S

In additi for most of the KRV conducted in th common land su ing able to collect fi cover was present. ven the inability rea (SCA), average r than aerially r, is in

assisting with the establishment of SAUs based on the variation of snow depths between land surface classes.

In mountain environments, there are many controls on snow depth, with some being more universally applicable than others. In this study, we chose aspect, elevation and canopy cover to classify and use as the basis for distinct SAUs. Even at a local or hill slope scale, the controls on snow depth distribution are complex and numerous (Pomeroy and Gray, 1995). However, the intent in this study is to identify general SAU properties that apply at the watershed scale. Greater snow accumulations tend to occur on north-facing slopes due to decreased levels of incoming solar radiation (Pomeroy and Gray, 1995; Anderton et al., 2004; Sicart et al., 2006), while a higher frequency and intensity of snowfall combined with decreased evaporation and melting generally lead to increasing snow depth with elevation (Pomeroy and Gray, 1995; Anderton et al., 2004). Increased canopy cover tends to reduce snow accumulation primarily due to canopy interception and sublimation (Hedstrom and Pomeroy, 1998; Pomeroy et al., 2002; Essery et al., 2003; Lpez-Moreno and Latron, 2008). Indeed, strong negative correlations between SWE and LiDAR-based forest canopy cover at forested sites in British Columbia have been demonstrated (Varhola et al., 2010).

Each of the three land surface types were stratified into appropriate classes based on observations in the LSDM and field data. These classes were then combined to derive unique S ow depths in areas spect and elevatio opy cover was com eturns (e.g., Barilotti While the SAU pro e capable of deriva in areas wher

Waters

Given th ailable bare earth Li d summar ties could then be ed. To

the 1:50,000 Canadian Digital Elevation Data (CDED) topographic map sheet DEMs were downloaded from the Natural Resources Canada Geobase web portal (www.geobase.ca). The spatial resolution of the CDED DEM was ten metres. LiDAR DEM and derivative properties are generally found to be superior to publicly available DEM data sources (e.g., CDED or USGS DEMs) but at coarse resolutions the elevation and basic terrain properties are comparable even over complex land covers and alpine terrain surfaces (Rayburg et al., 2009; Hopkinson et al., 2009).

Canopy cover was mapped from the canopy closure data layer within the Alberta Vegetation Inventory (AVI) produced by the Department of Sustainable Resource Development (SRD) Alberta. The AVI canopy closure attribute is derived by photo interpretation from medium resolution aerial photography (1:40,000 or 1:60,000) and stratified into four classes: 030%, 3150%, 51-70% and 71100% (Alberta Government, 2005). These class divisions are subjectively derived from data collected at different times to the LiDAR and summarized for forest stand polygons. Therefore, while the AVI canopy closure metric is analogous to that derived from LiDAR or digital hemispheric photography, it cannot be reliably compared due to spatial and temporal inconsistencies. Also LiDAR and DHP cover estimates are floating percentages from 0100%, while the AVI has already been aggregated to four discrete classes (Alberta Government, 2005). To facilitate a practical utilization of the AVI, while account for the dominant canopy cover influence, it was decided to classify the data into open and closed c %. This value was initi e AVI but was sub the ERW and KRV

The app d aspect, elevatio ominant sourc nean SAU snow tershed using SA to reconstr public data layers a impleme depth were generate late

spring melt period for the watershed outlet at Bragg Creek. Finally, A ten square kilometre section of one of the LSDM transects near the centre of the study area was reserved for comparison with the GIS extrapolated snow depths.

Results

Snow Depth

A summary of the good correspondence between LSDM and field data collected within KRV (including Marmot Creek) is illustrated in Figure 3. The average field depth was found to be 0.54 m (= 0.44 m), while the corresponding average LSDM value was 0.60 m (= 0.44 m). The bias and uncertainty varied by site and landcover but overall, the correlation between field and LSDM estimates demonstrates that average snow depths can be mapped within mountainous environments to within about a decimeter as long as care is taken to ensure alignment of the ground DEM and snow surface DSM. However, the field and LSDM data collected within the KRV area were expected to display increased depth values relative to comparable land surface classes in ERW due to the precipitation shadow effect as one travels east towards the foothills and prairie lands. The two closest and comparable active provincial snow course stations are Little Elbow (2225 m a.s.l.) in the headwaters of the ERW and Three Isle Lake (2170 m a.s.l.) immedia winter SWE for Little e (Alberta Governn

Figure 3 he KRV samplin on forested slopes; (e) Combined alpin 2011) [Note: fores city].

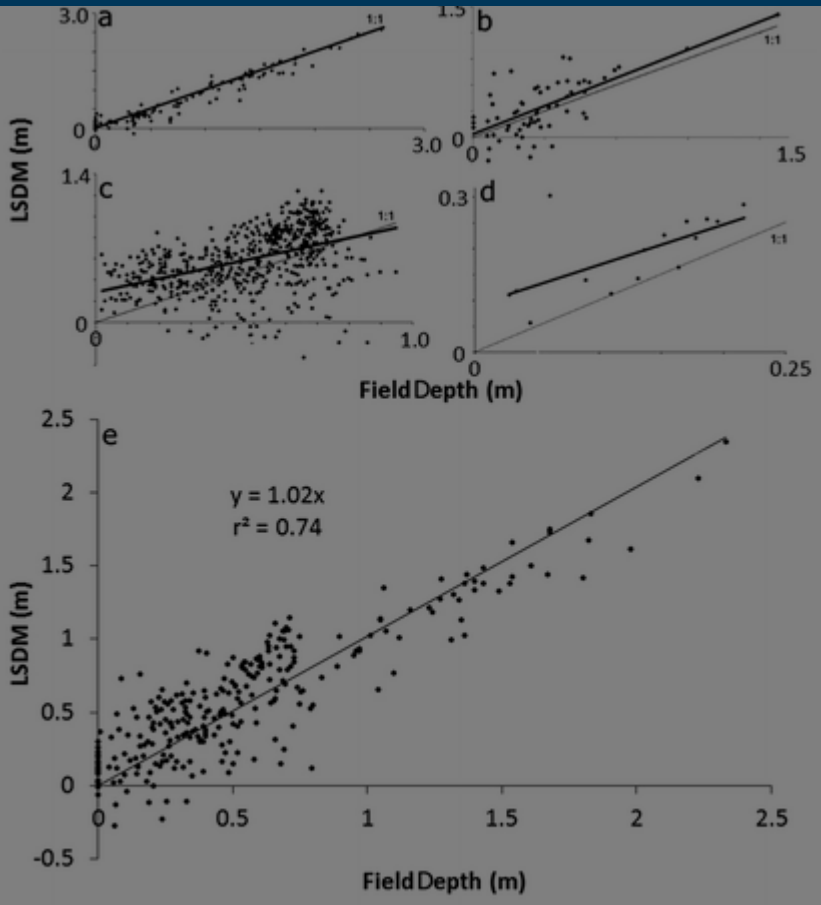

Figure 3. LSDM plotted against corresponding field measured depth within the KRV sampling locations: (a) alpine sites; (b) valley sites; (c) intermediate elevation forested slopes; (d) grouped snow depth standard deviations for the forested sites. (e) Combined alpine, forest slope and valley profiles are. (adapted from Hopkinson *et al.* 2011) [Note: forest slope data thinned by averaging (4:1) to reduce sample heteroscedacity].

Display full size

Stratified LSDM and field data for the ERW are illustrated in Figure 4a and 4b, respectively, and stratified LSDM data for the KRV are illustrated in Figure 4c. Overall, depths i at ERW, illustrati d above. The mea m). The mean LS > 0.05 m) was com free areas were co ing depth estimate llies. Inde n fill with snow u re these deep ac

Figure 4. onal cover, and terra e ERW. (b) Field sar cident LSDM results c

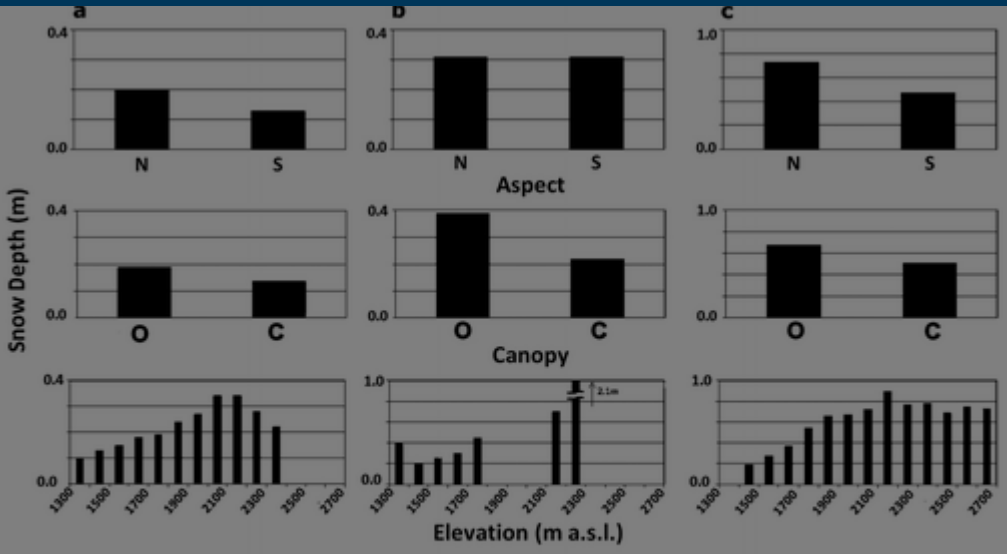

Figure 4. Snow depth sample data stratified by terrain aspect, canopy fractional cover, and terrain elevation. (a) LSDM results for sampling transects collected in the ERW. (b) Field sampling snow depth results collected in the ERW. (c) Temporally coincident LSDM results collected in the KRV area immediately west of the ERW.

Display full size

Apart from the already documented reduction in snow depth magnitude in eastern areas of the front ranges, similarity in LSDM behaviour at KRV and ERW is apparent when the data are stratified by north vs. south aspect, canopy cover and elevation (Figures 4a and 4c). North slopes possess deeper snow than south; open canopies illustrate deeper snow than closed canopies; and snow depth increases with elevation up to treeline. These observations are consistent with documented observations for northern hemisphere meso-scale watershed environments. The observation for snow depth to eline is redistrib er elevations by canop the treeline in this re which trap blowing Above treeline in the ERW, as the al ge there is sugg ile a decre s observed over the mediate adjacen the upper ERW is s treeline in the ERW

As expe aerially

LSDM represented all areas with and without snow cover (Figures 4a and 4b). As with the bulk field vs. LSDM estimate, the differences when the SCA was factored in reduced significantly and were well within the 0.27 m standard deviation observed in all field results. Both canopy cover and elevation stratifications of the field data illustrate the same general tendencies as observed in the LSDM. However, the north vs. south aspect stratification of the field data did not. This is due to field samples being collected in areas where snow accumulated and were readily accessible for measurement, and these areas tended to be nearer to the base of slopes, in forested or sheltered areas where aspect exerts less control. Therefore, in this case, the slope aspect stratification observed in the ERW and KRV LSDMs could be more reliable indicator of snowpack behaviour than the field data, as these results are not influenced by field access limitations.

Watershed SWE

Based on the above observations, ten unique SAUs were created from all plausible permutations of: north (27090) and south (90270) aspect; closed (>30%) and open (<30%) canopy cover; and low (<1700 m a.s.l.), medium (1700 >2200 m a.s.l.) and high (above treeline or >2200 m a.s.l.) elevation classes. [Note: above treeline, there is no canopy cover, so the two closed canopy classes for north and south facing slopes are redundant.] The LSDM depth data were stratified into these ten SAUs and used to train the

5).

Figure 5.

n units (SAUs) b

centre of watersh

pach.

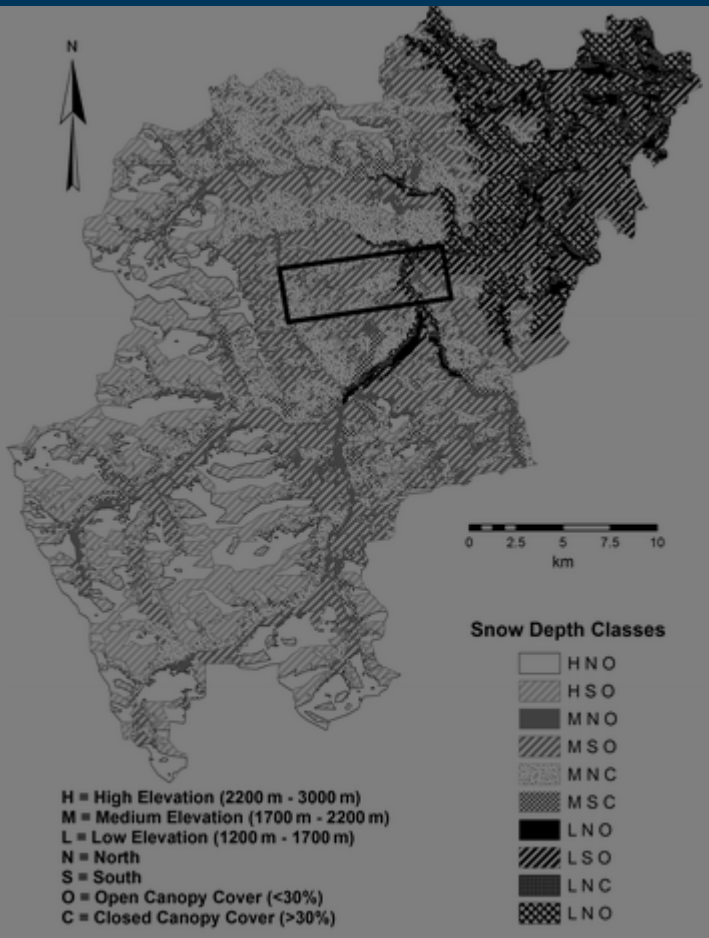

Figure 5. Classification scheme used to create 10 unique snow accumulation units (SAUs) based on elevation, aspect and canopy cover. Rectangular box near centre of watershed illustrates LSDM area used to test the spatial extrapolation approach.

Display full size

Depth integrated field snow density measurements ranged from 18 g cm^3 to 50 g cm^3 with a mean of 26 g cm^3 (= 8 g cm^3). There were no discernible elevation, aspect or canopy ed to convert depth to nsity to each of t estimate for the w pth distribut water resource s equivalent to 18% c on for 2008 (Env for 2008 (Figure 7 % that of the Albe e Little Elbow sn s self-evident eful long term pro or watersh greatly

Figure 6. Spatial distribution of estimated SWE across watershed.

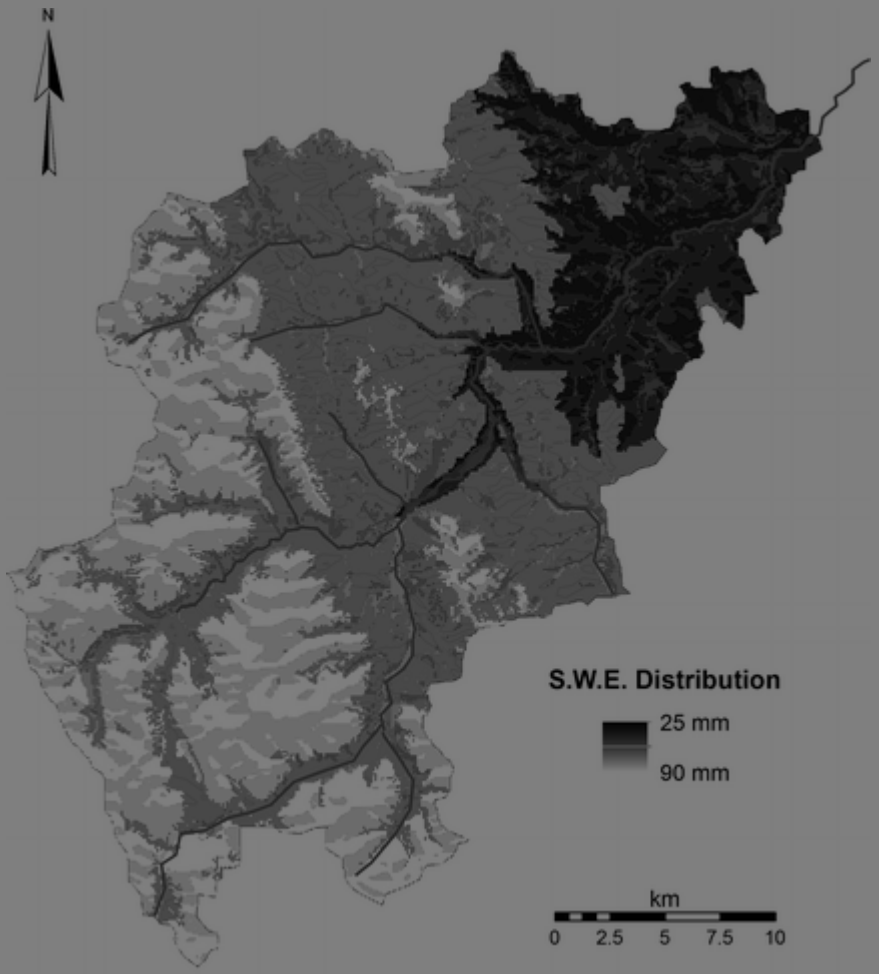

Figure 6. Spatial distribution of estimated SWE across watershed.

Display full size

Figure 7 ng winter SWE at L d of the Elbow Ri

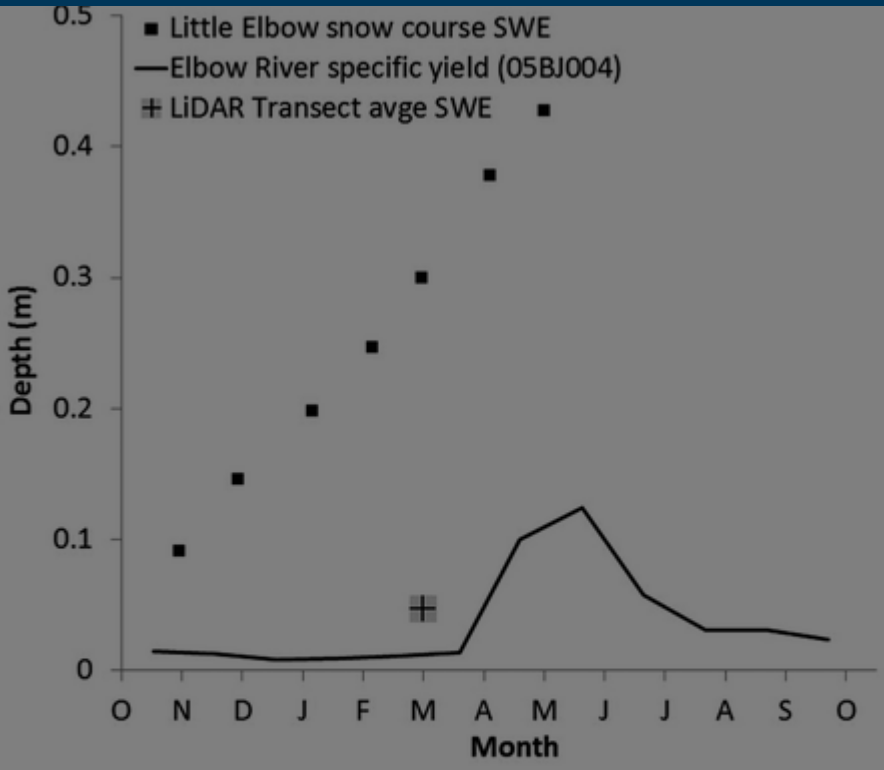

Figure 7. Estimated watershed SWE at end of March relative to the increasing winter SWE at Little Elbow snow course station (2200 m a.s.l.) and the specific yield of the Elbow River Watershed at Bragg Creek.

Display full size

The comparison of LSDM test data and GIS extrapolated snow depth across the full range of ten SAUs, indicated that while the correlation was reasonable (r^2 = 0.78), the GIS resu ercent near the cent are noticeab h within the watersh g the average mply apply the obse total watersh % reduction relat ore sophist e., land surface ally represer

Figure 8. now depth over all

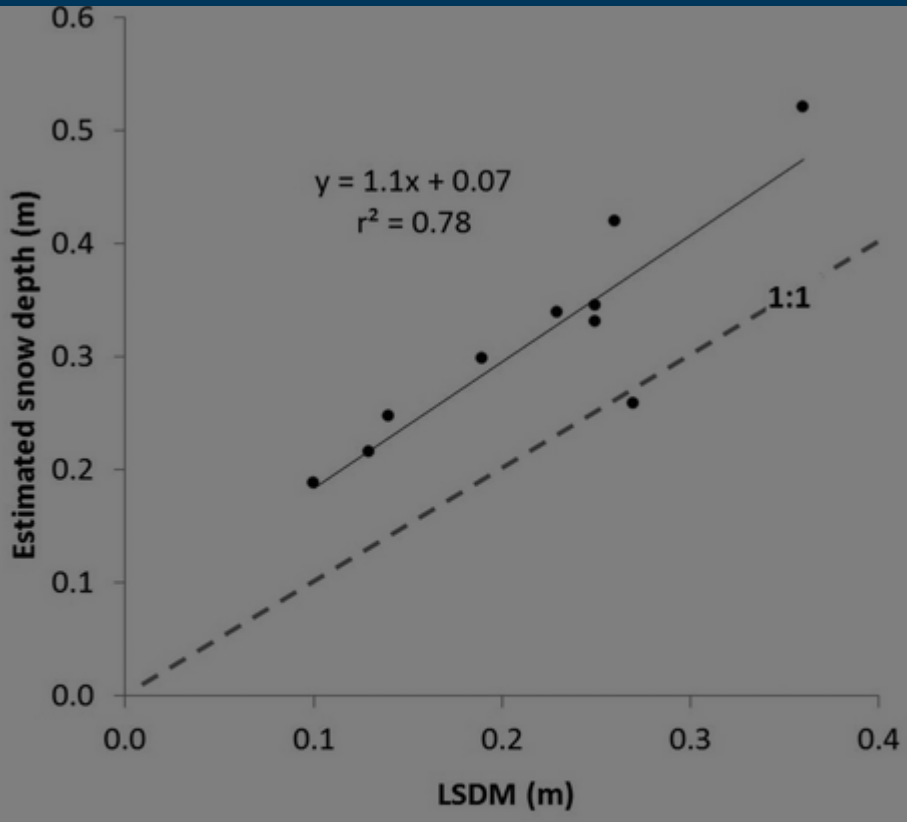

Figure 8. Comparison of GIS extrapolated snow depth with LSDM sampled snow depth over all 10 land surface classes with the test area.

Display full size

Discus

Field and tively dry
period w verage
LiDAR sn vered areas
only. By and
applying sources, an
estim geneous
terra LiDAR snow
depth as ly high. We
contend d surface
classes, und that
LiDAR es ents, tended
to slight on at the
KRV site SDM

Based on similar LSDM observations elsewhere, it has been reported that ground-level vegetation tends to systematically elevate true ground surface by up to ~0.1 m (Hopkinson et al., 2005), whilst snowpack surfaces, being highly reflective and smooth, tend to be more accurately represented in LiDAR data. The net effect is an under-estimation of snow depth in areas of dense ground level foliage. Steep terrain is known to introduce random errors into the surface elevation due to the propagation of horizontal uncertainty (Hodgson et al., 2005; Hollaus et al., 2006). A slope raster created from the 2006 LiDAR DEM indicated that only 1% of the surface exceeded 45. The proportional effect of these depth uncertainties, therefore, would be limited, and most likely there would be some compensation of under- and over-estimated depths. A cautionary note, however, is that steeper slopes tend to occur higher in the watershed on the western side, where snow depths are expected to be higher. Therefore, it might be reasonable to expect that random errors in depth would increase in those areas of alpine watersheds that typically experience deeper snowpack.

While individual LSDM grid-level values of several metres were observed in some areas and zero depths occurred over approximately 30% of the watershed, the mean depth of 0.26 m was approximately two times the manufacturer quoted 0.15 m accuracy for a single LiDAR data set (Optech Incorporated, 2005). A certain magnitude of error is to be expected even over perfectly flat and unambiguous ground or snow surfaces. In an extreme example, then, if both LiDAR ground and snowpack surfaces possessed equal but oppo with snow depths c depths of 0.3 m. A over and random f 0.26 m could co pondence displaye re within 0.02 m.

To ca DAR would require a d systema grid node of the LSD th of 0.26 m could co might not be statis DAR-based

impossible to quantify at what average snow depth the method provides results at a pre-determined level of confidence. However, given the types of bias and random behaviour discussed are likely to introduce uncertainties at the decimeter scale over most areas and potentially at the metre scale for small proportions (~1%) of the watershed, it is reasonable to assume that mean snow depths of approximately 1 m would produce reliable and useable results at a high level of confidence.

It was demonstrated that a relatively small spatial variation of <5 km in LiDAR depth observations led to the GIS results over-estimating the LSDM class-summaries by approximately 10% in the test area. The available base LiDAR data for LSDM creation was limited to the northern 40% of the watershed and had limited representation above tree line. While proxy data were available from the nearby Kananaskis River Valley area to provide some insight as to the expected snow depth patterns, it is known that snow depth can vary significantly at meso-scales (e.g., Elder et al., 1998). The controls on depth at the watershed scale are not always localized and can vary due to synoptic meteorological variations, orographic and precipitation shadow effects. Therefore, by having no sample representation in the southern part of the watershed, this created an unquantifiable level of uncertainty in the SWE estimate generated. If this method of snowpack water resource assessment were to be used in an operational setting, a more spatially complete base LiDAR coverage would be required to enable sampling over appropriately spaced and representative land surface classes covering the full geograp nsects would ne ons but far enough erial coverag (altitude, swath w

Con

Despite emonstrated a remote source assessm d surface classifica nsects shows p w depth

reduced need for field personnel deployment combined with spatially explicit and rapid (within two to three days of acquisition) estimations of snowpack depth and volume at the meso-scale. This relatively simple approach to snowpack monitoring could be of significant value to water resource managers when accurate and repeatable estimates of the spring runoff volume are needed for seasonal water supply, irrigation and power generation forecasts, as well as flood risk assessment.

At the current time it is not thought that the approach to snowpack monitoring described in this study is sufficiently cost-effective or accurate for operational water resource monitoring. However, the speed, aerial coverage, accuracy and costs of airborne LiDAR data have all improved greatly in recent years and continue to do so. Therefore, given growing water scarcity and potential flood risk challenges in parts of the Bow River basin, it is possible that the need for more accurate spatial estimates of headwater snowpack volumes will make the investment in LiDAR snow sampling worthwhile at sometime in the next decade. Indeed, active snow course monitoring already requires helicopters to transport snow monitoring crews and the Alberta LiDAR base coverage is gradually heading towards completion (Airborne Imaging, 2010). Therefore, it will soon be feasible to mount a small and cost effective LiDAR profiling sensor on the helicopter so that snow depth transects could be automatically collected en route between snow course sites. While there would be a cost associated with the hardware and the post-processing, the actual operational costs would be little to no more tha

Acknow

The City d for funding this proj provided by the C tural Scien ment and Alberta n, helicopt thank Wolf Survey a of survey equipme Diiwu is acknowl Beer and

and James Churchill provided valuable assistance in the field. We are also grateful to Airborne Imaging Inc. for flying the 2008 snowpack LiDAR survey on a cost-recovery basis. Mike Demuth, Geological Survey of Canada, and the Canadian Consortium for LiDAR Environmental Applications Research provided aviation support in 2007.

References

1. Airborne Imaging. 2010. Airborne Imaging LiDAR coverage of Western Canada.http://www.airborneimaginginc.com/Maps/Canada_coverage_maps/Airborne_Library_Coverage.pdf (accessed February 2011). http://www.airborneimaginginc.com/Maps/Canada_coverage_maps/Airborne_Library_Coverage.pdf
Google Scholar

2. Alberta Government. 2005. Alberta Vegetation Inventory Interpretation Standards, Version 2.1.1, Chapter 3: Vegetation Inventory Standards and Data Model Documents. Resource Information Management Branch, Alberta Sustainable Resource Development, 99 pp. http://www.srd.alberta.ca/LandsForests/documents/AVI-ABVeg
Goog

3. Albert ankings for the Bo Basin. crank.pdf (acces
G

4. Ander variability in snow esses , 18 : 435 –

Article contents | Related research

5. Axelsson , P. 1999 . Processing of laser scanner data algorithms and applications . ISPRS Journal of Photogrammetry and Remote Sensing , 54 : 138 – 147 .
Web of Science ® | Google Scholar

6. Baltsavias , E. P. 1999 . Airborne laser scanning: Basic relations and formulas . ISPRS Journal of Photogrammetry and Remote Sensing , 54 : 199 – 214 .
Web of Science ® | Google Scholar

7. Barilotti, A., S. Turco, and G. Alberti. 2006. LAI determination in forestry ecosystems by LiDAR analysis. Workshop on 3D Remote Sensing in Forestry, 14-15/02/2006, BOKU Vienna.
Google Scholar

8. Boon , S. 2007 . Snow accumulation and ablation in a beetle-killed pine stand, northern Interior British Columbia . BC Journal of Ecosystems and Management , 8 (3) : 1 – 13 .
Google Scholar

9. Coops , N. C. , Varhola , A. , Bater , C. W. , Teti , P. , Boon , S. , Goodwin , N. R. and Weiler , M. 2010 . Assessing differences in tree and stand structure following beetle infesta 6) : 497 – 508 .

10. DeBee off contri iences , 14 : 1205 -

11. Deem Accuracy and e USA, 33033
Goog

12. Deems , J. S. , Fassnacht , S. R. and Elder , K. J. 2006 . Fractal distribution of snow depth from LiDAR data . Journal of Hydrometeorology , 7 : 285 – 297 .
Web of Science ® | Google Scholar

13. Derksen , C. , Walker , A. and Goodison , B. 2005 . Evaluation of passive microwave snow water equivalent retrievals across the boreal forest-tundra transition of western Canada . Remote Sensing of Environment , 96 : 315 – 327 .
Web of Science ® | Google Scholar

14. Elder , K. J. , Rosenthal , W. and Davis , R. E. 1998 . Estimating the spatial distribution of snow water equivalence in a montane watershed . Hydrological Processes , 12 : 1793 – 1808 .
Web of Science ® | Google Scholar

15. Environment Canada. 2009. Hydat: Archived hydrometric data. Available online: http://www.wsc.ec.gc.ca/hydat/H2O/index_e.cfm (accessed January 2010).
http://www.wsc.ec.gc.ca/hydat/H2O/index_e.cfm
Google Scholar

16. Essery , R. L. H. , Pomeroy , J. W. , Parviainen , J. and Storck , P. 2003 . Sublimation of snow
16 : 1855 – 1864 .

17. Fassna
ling for deep monta

18. Fisera
f Marmot Creek
dings, eds. R. H. S
Edmonton, AB, Re
Goog

19. Goulden , T. and Hopkinson , C. 2010 . The forward propagation of integrated system components within airborne LiDAR data . Photogrammetric Engineering and Remote Sensing , 76 (5) : 598 – 601 .
Web of Science ® | Google Scholar

20. Greene , E. M. , Liston , G. E. and Pielke , R. A. 1999 . Simulation of above treeline snowdrift formation using a numerical snow-transport model . Cold Regions Science and Technology , 30 : 135 – 144 .
Web of Science ® | Google Scholar

21. Hedstrom , N. R. and Pomeroy , J. W. 1998 . Measuring and modeling of snow interception in the boreal forest . Hydrological Processes , 12 : 1611 – 1625 .
Web of Science ® | Google Scholar

22. Hodgson , M. E. and Bresnahan , P. 2004 . Accuracy of airborne lidar-derived elevation: Empirical assessment and error budget . Photogrammetric Engineering and Remote sensing , 70 : 331 – 340 .
Web of Science ® | Google Scholar

23. Hodgson , M. E. , Jensen , J. , Raber , G. , Tullis , J. , Davis , B. A. , Thompson , G. and Schuc ain slope in leaf-of 60 : 817 – 823 .

24. Hollau f large scale canop a complex al ng , 60 : 323 –

25. Hopki bfleisch , W. and Tr levation and canop rnal of

Web of Science ® | Google Scholar

26. Hopkinson , C. and Demuth , M. D. 2006 . Using airborne LiDAR to assess the influence of glacier downwasting to water resources in the Canadian Rocky Mountains . Canadian Journal of Remote Sensing , 32 : 212 – 222 .
Web of Science ® | Google Scholar

27. Hopkinson , C. , Hayashi , M. and Peddle , D. 2009 . Comparing alpine watershed attributes from lidar, Photogrammetric, and Contour-based Digital Elevation Models . Hydrological Processes , 23 : 451 – 463 .
Web of Science ® | Google Scholar

28. Hopkinson, C., J. Pomeroy, C. DeBeer, C. Ellis, and A. Anderson. 2011. Relationships between snowpack depth and primary LiDAR point cloud derivatives in a mountainous environment. In Proceedings of Remote Sensing and Hydrology. Jackson Hole, Wyoming, USA, September 2010, IAHS Publ. 3XX, 2011.
Google Scholar

29. Hopkinson , C. , Sitar , M. , Chasmer , L. E. and Treitz , P. 2004 . Mapping snowpack depth beneath forest canopies using airborne LIDAR . Photogrammetric Engineering and R

30. Keckle den, Colora
Goog

31. Le 2005 . Metho n digital hemis eorology , 129 :

32. Lpez-M ow

Web of Science ® | Google Scholar

33. Martz, L., J. Bruneau, and J. T. Rolfe. 2007. Climate change and water; SSRB final technical report. 252 pp. (http://www.usask.ca/geography/giservices/images/SSRB_Final_Report.pdf) (accessed February 2011). http://www.usask.ca/geography/giservices/images/SSRB_Final_Report.pdf Google Scholar

34. Minoru , A. and Hiroshi , S. 2006 . Snow depth derived from airborne LIDAR data and estimation of snow water equivalent volume . Journal of Japan Society of Photogrammetry and Remote Sensing , 45 : 24 – 33 . Google Scholar

35. Musselman , K. N. , Molotch , N. P. and Brook , P. D. 2008 . Effects of vegetation on snow accumulation and ablation in a mid-latitude sub-alpine forest . Hydrological Processes , 22 : 2767 – 2776 . Web of Science ® | Google Scholar

36. Optech Incorporated. 2005. ALTM 3100 specifications. Toronto, Ont.: Optech Incorp
Goog

37. Pentn The water
manag nadian
Water

38. Permit iver basin to
new w Resources
Journa

39. Pomer ment. NHRI

Google Scholar

40. Pomeroy , J. W. , Gray , D. M. , Hedstrom , N. R. and Janowicz , J. R. 2002 . Prediction of seasonal snow accumulation in cold climate forests . Hydrological Processes , 16 : 3543 – 3558 .
Web of Science ® | Google Scholar

41. Province of Alberta. 2007. Bow, Oldman and South Saskatchewan River basin water allocation order. Alberta Regulation 171/2007, Water Act.
Google Scholar

42. Rayburg , S. , Thoms , M. and Neave , M. 2009 . A comparison of digital elevation models generated from different data sources . Geomorphology , 106 (34) : 261 – 270 .
Google Scholar

43. Sicart , J. E. , Pomeroy , J. W. , Essery , R. L. H. and Bewley , D. 2006 . Incoming longwave radiation to melting snow: Observations, sensitivity and estimation in northern environments . Hydrological Processes , 20 : 3687 – 3708 .
Web of Science ® | Google Scholar

44. Trujillo gic, and canop f snow depth

45. Valeo . Climate ch s Journal , 32 (4

46. Varhol M. 2010 . The in ow accum st Research ,

Web of Science ® | Google Scholar

47. Wehr , A. and Lohr , U. 1999 . Airborne laser scanning-an introduction and overview . ISPRS Journal of Photogrammetry and Remote Sensing , 54 : 68 – 86 .
Web of Science ® | Google Scholar

48. Winkler , R. and Boon , S. 2010 . The effects of mountain pine beetle attack on snow accumulation and ablation: A synthesis of ongoing research in British Columbia . Streamline Watershed Management Bulletin , 13 (2) : 25 – 31 .
Google Scholar